Improvement of Shaped Conductive Backfill Material for Grounding Systems

Run Xiong [1], Qin Yin [1], Wen Yang [2], Yan Liu [1], and Jun Li [1]

[1] PLA Army Engineering University, Nanjing 210007, Jiangsu, China
xiongrun1983@sina.com, yinqin1983@139.com, 76077381@qq.com, 3459990149@qq.com

[2] PLA Army Research Institution, Kunming, Yunnan 650222, China
76077381@qq.com

Abstract ─ In this paper, some improvements have been proposed for low resistance shaped conductive backfill material (SCBM) based on finite-difference time-domain (FDTD) simulations in grounding systems. It is found SCBM can be produced by conjunction of several layers with conductivity decreasing gradually from inner layer to outer layer, and smooth conductivity reduction between layers would lead to a better grounding performance. It is also found cuboid shape is a much more efficient shape than cube and cylinder shapes for SCBM, and holes can be made on the SCBM's main body. It suggested to bury SCBM vertically when ground soil permits, otherwise bury SCBM horizontally and deeper burying depth would result in smaller grounding resistance. Results show it is not needed to connect the SCBMs one by one tightly in series SCBM, and some distances is allowed without dramatically increasing grounding resistance.

Index Terms ─ Finite-difference time-domain (FDTD) method, shaped conductive backfill material (SCBM), transient grounding resistance (TGR).

I. INTRODUCTION

Grounding system plays an important role in lightning protection systems. When lightning strikes, the overvoltage is dependent on the grounding system resistance and a lot of papers have been published on efforts to reduce the system's grounding resistance [1-3].

Low resistance shaped conductive backfill material (SCBM), increases the grounding and soil contact area and thus decreases the grounding system's resistance. SCBM can be widely used in various grounding systems, especially to areas of high soil resistivity, to reduce grounding resistance and ensure long-term stable grounding effect without resulting huge cost rise [4-5].

Besides experimental analyses [6-8], numerical simulations have been widely used in lightning protection grounding systems design [8-11]. The finite-difference time-domain (FDTD) method [12-14], which provides a simple and efficient way of solving Maxwell's equations for a variety of problems, has been usually used to evaluate grounding system performance.

In [15], some optimal programs have been proposed for SCBM to be used in lightning protection systems. In this paper, some additional improvements are proposed for SCBM in the grounding system. Firstly, to simplify the production of the linear or parabolic type varied conductivity SCBM in Section D of Part III in [15], layered SCBM's performance, whose conductivity decreases gradually from the inner layer to the outer layer, is studied. Secondly, shape effect of SCBM on resistance is studied to find out the optimized shape to reduce high conductivity material usage in the SCBM production, and in this paper three typical shapes are involved, which are cube, cylinder and cuboid SCBMs. Thirdly, square and round holes are made on the SCBM main body to further reduce high conductivity material usage, and both field distribution and transient grounding resistance (TGR) are monitored to find out the holes effect on the SCBM performance. Fourthly, the performance of vertically buried SCBM is compared with that of horizontally buried SCBM with the same size to learn the SCBM position's effect on TGR. Lastly, series SCBM's performance is studied, and both field distribution and TGR are monitored to derive some suggestions on the distance between neighboring SCBMs in the series SCBM. Based on these analyses, some improvements are proposed for SCBM in grounding systems.

II. TGR CALCULATION MODEL

To improve SCBM programs of grounding system, the TGR calculation model proposed in [15] is adopt as shown in Fig. 1. It worth to note that the in Fig. 1, CPML stands for Convolutional Perfectly Matched Layer [16], and PEC stands for Perfect Electric Conductor which is used to truncate the CPML. A homogenous ground, whose relative permittivity is $\varepsilon_g=10\varepsilon_0$ and conductivity is $\sigma_g=0.004$ S/m, is adopted.

Submitted On: November 23, 2020
Accepted On: February 19, 2021

https://doi.org/10.47037/2020.ACES.J.360410

1054-4887 © ACES

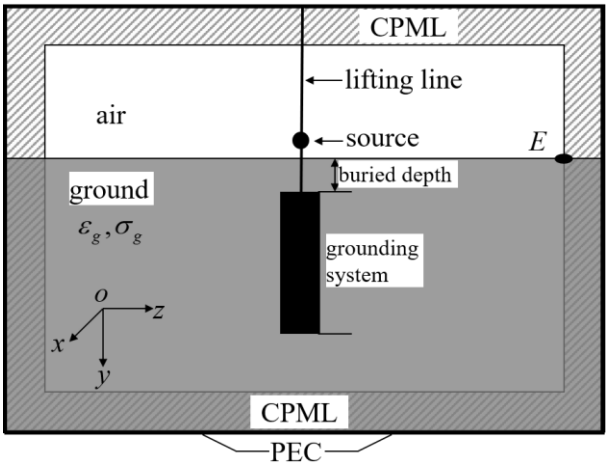

Fig. 1. TGR simulation model.

The lightning restrike current is injected 200 mm above ground through, which is modeled by:

$$\boldsymbol{I}(t) = I_0(e^{-\alpha t} - e^{-\beta t}), \quad (1)$$

where I_0=109405 A, α=22708 s^{-1}, β=1294530 s^{-1}.

The TGR is defined as a ratio of the transient voltage to the transient current:

$$R_t = V_t / I_t. \quad (2)$$

Here I_t is the transient current flowing through the grounding system, which can be defined from the Ampere circuital theorem as shown in [17]:

$$I(t) = [H_z(i_0 - \tfrac{1}{2}, j_0 - \tfrac{1}{2}, k_0) - H_z(i_0 + \tfrac{1}{2}, j_0 - \tfrac{1}{2}, k_0)]\pi\Delta_z / 4 + [H_x(i_0, j_0 - \tfrac{1}{2}, k_0 + \tfrac{1}{2}) - H_x(i_0, j_0 - \tfrac{1}{2}, k_0 - \tfrac{1}{2})]\pi\Delta_x / 4, \quad (3)$$

where (i_0, j_0, k_0) is the point where the lifting line entering ground.

The transient voltage V_t can be obtained from:

$$V_t = \sum_{k=N_l}^{N_A} V_j = -\sum_{k=N_l}^{N_A} E_z(i_0, j_0, k)\Delta_z, \quad (4)$$

where $E_z(i_0, j_0, k)$ is the electric field in the z direction in the air-ground interface plane, N_l and N_A are FDTD mesh indexes of the point (i_0, j_0, k_0) and point "E" in Fig.1 respectively.

All simulation is carried out on a PC with the parameter below:

Pentium IV 2.8GHz CPU per Node,
2.0GBytes Memory per Node,
1000M High-speed Network Interface Card,
1000M Bites Switch.

III. OPTIMIZED PROGRAMS FOR SCBM

In this part, several proposed programs are tested to derive some efficient improvements for SCBM in grounding system.

A. The layered SCBM

As pointed out in Section D of Part III in [14], TGR of SCBM whose conductivity is linear or parabolic type varied, can be as low as the resistance of a totally high conductivity SCBM. However, it is not easy to produce continuous varied conductivity SCBM in practice, thus layered SCBM is proposed. The permittivity in each layer is the same, but the conductivity decreases gradually from the inner layer to the outer layer.

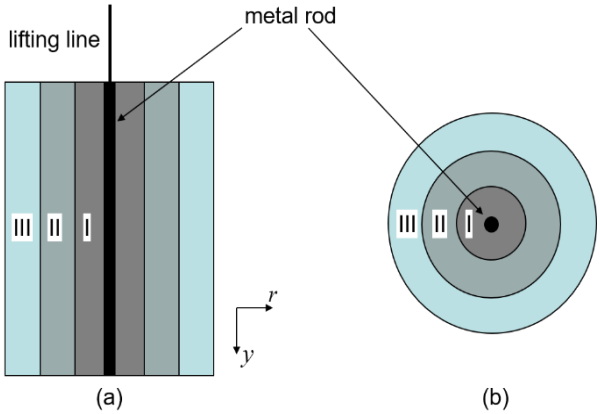

Fig. 2. Layered cylinder SCBM.

In this section, a 2-D cylindrical coordinate area of the proposed TGR calculation area in part IV of [15] is occupied, and the SCBM dimension is the same as that in [15]. The cylinder SCBM is produced into three layers, as shown in Fig. 2.

The cylindrical SCBM is 150 mm in radius and 800 mm in length, and the metal rod radius is 5 mm. Here the main body of SCBM is divided into three layers, and the inner layer (layer I) radius is 45 mm and the outer two layers (layer II and III) are both 50 mm in radius.

Two cases of layered SCBMs are tested here, where conductivity decreases more smoothly in case II than case I, and the conductivity of the two SCBMs decreases from inner layer to the outer layer gradually. The conductivity of the two cases are listed in Table 1, and the relative permittivity in the three layers are all set at ε_s=10.0.

Table 1: Conductivity of the three layered SCBM

	Layer I	Layer II	Layer III
Case I	0.5 S/m	0.1 S/m	0.02 S/m
Case II	0.5 S/m	0.2 S/m	0.08 S/m

The computational grid size is $\Delta=\Delta_r=\Delta_z$=5 mm and the time step is $\Delta t=\Delta/2c$, where c is the speed of light. The simulation is carried out 240000 time steps, which equals to 2 ns, and the TGR is calculated through (2).

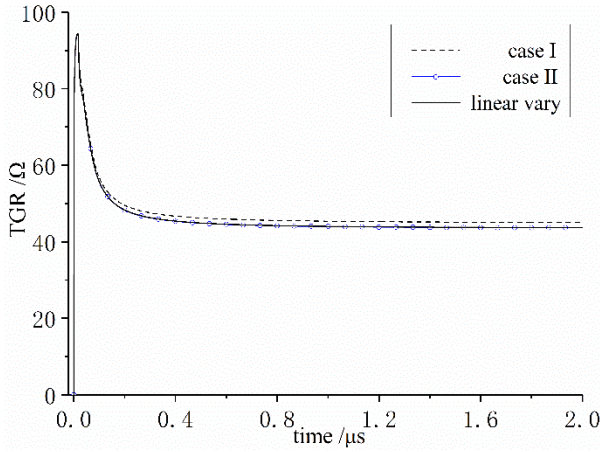

Fig. 3. TGRs of the layered SCBM compared with liner varied conductivity SCBM.

In Fig. 3 is graphed the TGRs of the two cases of layered SCBM, where the TGR of linear varied conductivity SCBM given by (8) of [15] is also presented for comparison. It can be seen that the three SCBMs has similar early performance from 0 to 0.05 μs, while performance varies after 0.05 μs. The steady grounding resistance is 45.06 Ω for case I and 43.70 Ω for case II, compared with 43.66 Ω for linear varied SCBM. It is clear that the layered SCBM of case II performs similarly as the linear varied SCBM. Thus, it can be concluded SCBM can be produced into several layers with conductivity decreasing gradually from inner layer to outer layer, and smooth conductivity reduction between layers would result in a better grounding performance.

B. SCBM shape effect on TGR

SCBM can be made into different shapes, but how SCBM shape will affect the grounding performance have not been studied, thus it is needed to test shape effect on SCBM's TGR. In this section, three typical SCBMs are tested, as shown in Fig. 4. The lengths of the three SCBMs are all 800 mm in this section, and buried vertically with the upper side of the SCBMs 500 mm below the air-ground interface. To

In Fig. 4 (a) is the sectional dimension of the cube SCBM, which is 150 mm in each direction, the sectional area is 2.25×10^4 mm^2. In Fig. 4 (b) is graphed the sectional dimension of cylinder SCBM, whose radius is 85 mm and the sectional area is 2.27×10^4 mm^2. In Fig. 4 (c) is graphed the sectional dimension of the cuboid SCBM, which is 380 mm×60 mm and the sectional area is 2.28×10^4 mm^2. To simulate the problem with less computational error introduced by three dimensional cubic FDTD cell modelling, cube metal rod is occupied here. Cylinder SCBM in Fig. 4 (b) is simulated by conformal grids [12]. It is worthy of noting that the sectional area of the three SCBMs is close to each other, which means similar material will be consumed in the production of the three SCBMs.

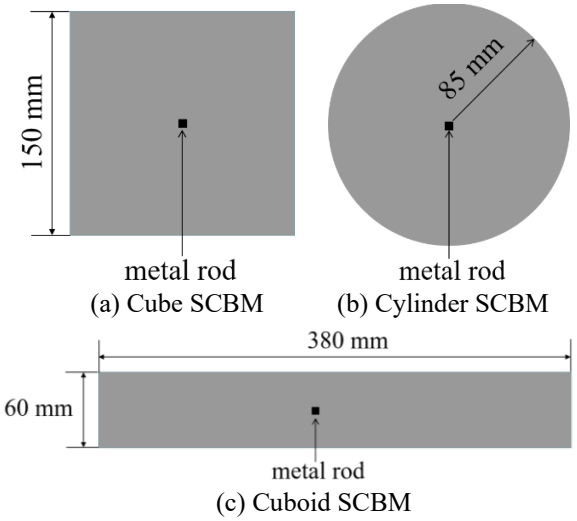

Fig. 4. Typical SCBM shapes tested.

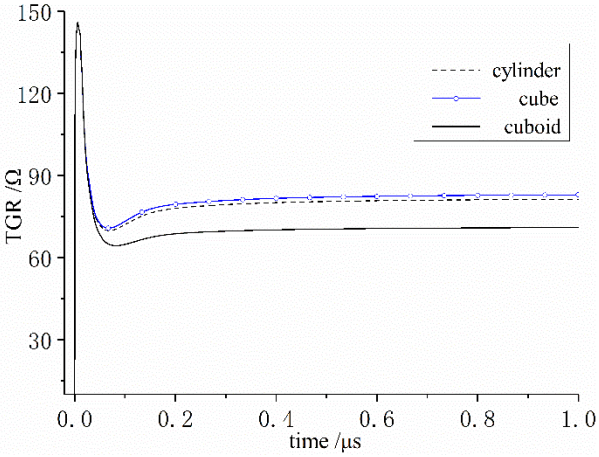

Fig. 5. TGRs of three typical shape SCBM.

In this section and below, three dimensional FDTD simulations are occupied. The computational grid size is $\Delta=\Delta_x=\Delta_y=\Delta_z=5$ mm and the time step is $\Delta t=\Delta/2c$, where c is the speed of light. The simulation is carried out 120000 time steps, which equals to 1 μs, and TGR of SCBMs are calculated through (2). TGR of the three SCBMs in Fig. 4 is simulated and graphed in Fig. 5.

From Fig. 5, it can be seen that the three SCBMs has similar early performance from 0 to 0.05 μs, however varies after 0.05 μs. The steady resistance is 81.31 Ω for cylinder SCBM, 82.91 Ω for cube SCBM, and 70.86 for cuboid SCBM. Thus, it can be concluded cuboid shape is a more efficient shape for SCBM which can result in smaller grounding resistance at similar high conductivity material usage.

C. Holes on SCBM main body

To test effect of holes on the SCBM main body on TGR, two SCBMs with four penetrating square holes on each SCBM are tested, and sectional dimensions are shown in Fig. 6. Vertically cube buried SCBM is adopted in this section, whose size is 150 mm×150 mm×800 mm, and buried 500 mm below ground. The four square holes are located symmetrically on SCBM main body, and the distance between two neighboring holes is 30 mm. The square hole's width is 25 mm and 35 mm for the two SCBMs respectively. It worth to note that the four holes are filled with ordinary soil when buried, and the relative permittivity of ground is ε_r=10.0 and the conductivity is σ_g=0.004 S/m.

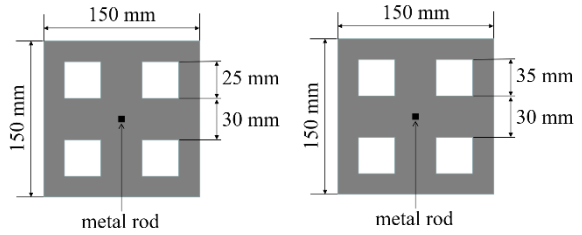

(a) SCBM with 4×25mm holes (b) SCBM with 4×35mm holes

Fig. 6. SCBM with different size holes.

To analyze the holed SCBM's performance, we monitored electric field component distribution firstly, as shown in Fig. 7. It is worthy of noting that the SCBM locates at the center of the two figures, that is $x \in$ (-7.5 mm, 7.5 mm), $z \in$ (-7.5 mm, 7.5 mm). In Fig. 7 is showed the horizontal electric field E_h in *xoz* plane, which is given by:

$$E_h(x,z) = \sqrt{E_x^2(x,z) + E_y^2(x,z)}\,, \tag{5}$$

where $E_x(x, z)$ and $E_z(x, z)$ are the electric field component in x and z direction in *xoz* plane respectively. Since electric fields located at half space steps in FDTD. It worth to note that $E_x(x, z)$ is get from $\frac{1}{2}(E_x(x+\frac{\Delta_x}{2}, z) + E_x(x-\frac{\Delta_x}{2}, z))$ and $E_z(x, z)$ is get from $\frac{1}{2}(E_z(x, z+\frac{\Delta_z}{2}) + E_z(x, z-\frac{\Delta_z}{2}))$.

It can be seen from Fig. 7 that electric field in the SCBM main body is lower than the surrounding area, and the electric field at the four corners of the cube SCBM is much higher than other places. In the SCBM main body, the electric field increases from the center to the outer edge. It can also be seen that lightning current flows from the SCBM to the surrounding areas and amplitude decreases as the distance from SCBM edge increases. The electric field in the SCBM is much lower than surrounding soil, which demonstrates SCBM performs well to conduct lightning electricity. However, electric field component E_h distributes continuously in the SCBM main body even though there are four holes located, and the holes are not visible in Fig. 7, which means effect of holes on SCBM's current-carrying capacity is limited.

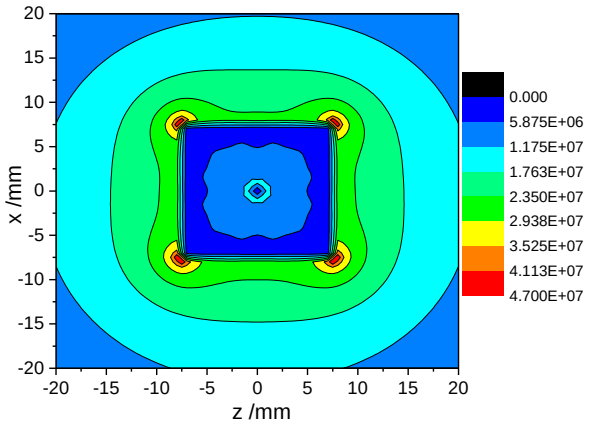

Fig. 7. E_h distribution in *xoz* plane.

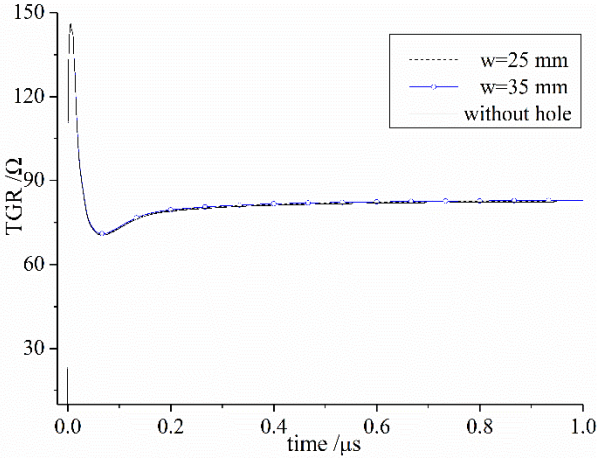

Fig. 8. TGR of SCBMs with different size square holes.

Besides field distribution, we also monitored TGRs of the two SCBMs, as shown in Fig. 8, where the TGR of a same size SCBM without any hole on the main body is also presented as reference. From Fig. 8, it can be seen that TGR is nearly the same for the two SCBMs with holes. The steady resistance for the SCBM shown in Fig. 6 (a) is 82.71 Ω, and 82.93 Ω for the SCBM shown in Fig. 6 (b), compared with 82.40 Ω for a same size SCBM without any hole.

Additionally, we also tested round holes effect on SCBM's TGR. Two size holes are simulated here, as shown in Fig. 9. In Fig. 9 (a) is shown the SCBM where radius of the four holes is 20 mm and the distance between two neighbouring holes is 40 mm; while in Fig. 9 (b) is the SCBM where radius of the four holes is 30 mm and the distance between two neighbouring holes

is 20 mm.

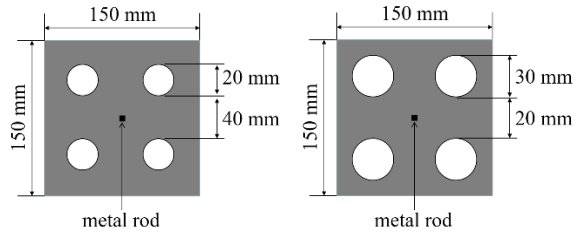

(a) Radius of the 4 holes is 20mm (b) Radius of the 4 holes is 30mm

Fig. 9. SCBM with different size holes.

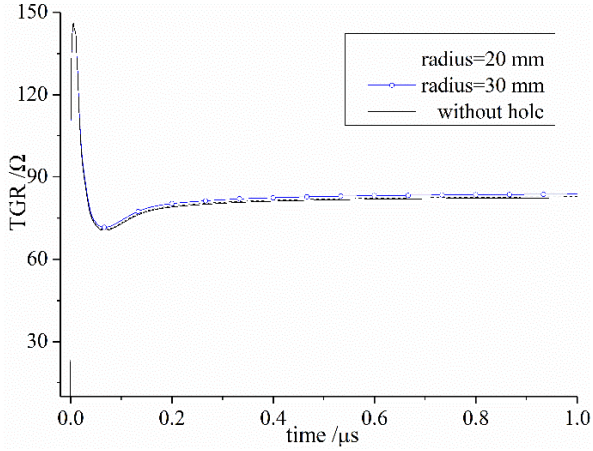

Fig. 10. SCBM with different radius round holes.

Figure 10 graphs TGRs of the two SCBMs shown in Fig. 9, where the TGR of a same size SCBM without any holes on the main body is also presented as reference. It can be seen that there is mild difference between TGRs of the two SCBMs with holes. The steady resistance for the SCBM of Fig. 9 (a) is 82.78 Ω, and 83.70 Ω for the SCBM of Fig. 9 (b), compared with 82.40 Ω for a same size SCBM without any hole. From the analyses in this section, it can be concluded that holes can be made on SCBM main body to reduce high conductivity material usage.

D. Vertically buried versus horizontally buried

At some places it may be costly to dig deep enough to bury SCBM vertically, so it is needed to evaluate the cost and SCBM buried position. To study the SCBM buried position effect, we compared TGRs of a same SCBM buried vertically versus horizontally. The dimension of the SCBM is 380 mm×60 mm×800 mm, and two burying depths are tested. The horizontally buried SCBM is as shown in Fig. 11, where *d* is burying depth of SCBM's upper side below ground. The burying depth is *d*=500 mm and *d*=1300 mm respectively here. The upper side depth of the vertically buried SCBM is 500mm, and the down side depth is 1300 mm. TGRs of the three cases are monitored as shown in Fig. 12.

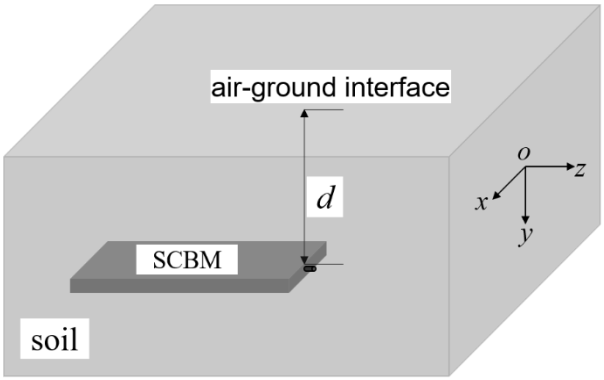

Fig. 11. The horizontally buried SCBM.

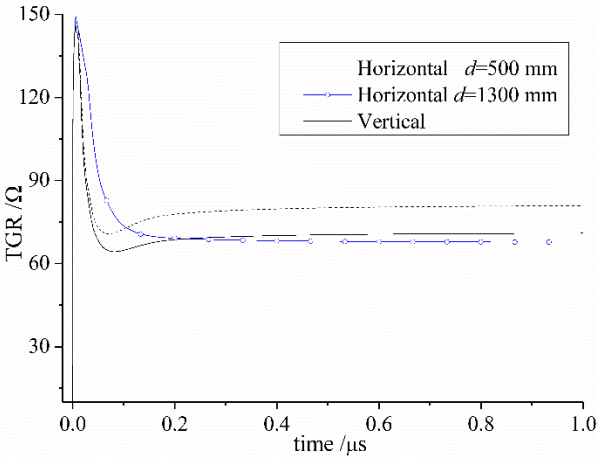

Fig. 12. Resistance of horizontally buried SCBMs.

From Fig. 12, it can be seen that the horizontally buried SCBMs' performance is quite different from the vertically buried one. The steady resistance of the horizontally buried SCBM is 80.89 Ω when *d*=500 mm, and 67.75 Ω when *d*=1300 mm, compared with 70.96 Ω for the vertically buried SCBM. From comparison of horizontally buried SCBM with vertically buried SCBM at the same depth *d*=1300 mm, there is only a 2.21 Ω resistance improvement for horizontal position, but that would result in a quite larger amount of soil excavation in construction. Thus, it suggested to bury SCBM vertically when ground soil permits, otherwise bury SCBM horizontally and greater depth of the horizontally buried SCBM would result in smaller resistance, but the effect of increasing the buried depth on the resistance reduction is limited.

Fig. 13. Series SCBM to be buried.

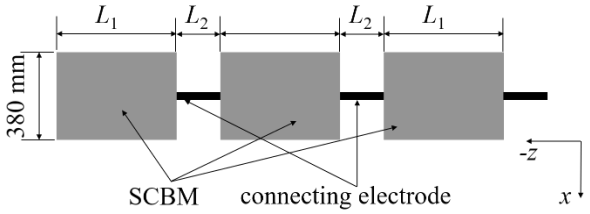

Fig. 14. Dimension of series SCBM.

Table 2: Parameters of 5 Series SCBM

	Case I	Case II	Case III	Case IV	Case V
L_1 (mm)	450	350	475	275	5000
L_2 (mm)	50	150	150	250	0
n (number)	10	10	8	8	1

E. Series SCBM performance

To get a low-level grounding resistance, SCBMs are connected horizontally into series SCBM in practice, as shown in Fig. 13. However, the series SCBM performance has yet been studied. In this section, the metal rod of SCBMs is connected one by one to make a series SCBM and grounding resistance is studied as the SCBM numbers and distance between SCBMs varies. It worth to note that to avoid the grounding system's effect on the accuracy of the simulated TGR as pointed out in [17], the series SCBM are buried in the –z direction, whereas the transient voltage V_t in (4) is integrated in +z direction. The series SCBM is connected to lifting line at x=0 mm, z=0 mm.

The total length of the series SCBM is 5 m, and all the SCBMs are of the same size for each case. The length of each SCBM is L_1 and the distance between two neighbouring SCBMs is L_2, as shown in Fig. 14. In all cases, the SCBMs are 380 mm in width and 60 mm in depth, but length L_1 varies. The SCBMs are connected by metal connecting electrodes with sectional dimension 10 mm×10 mm, and the series SCBM is buried 300 mm below the ground surface.

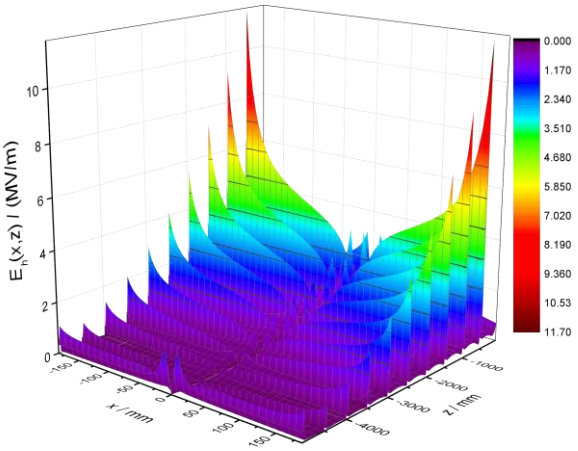

Fig. 15. $E_h(x, z)$ distribution in the series SCBM area.

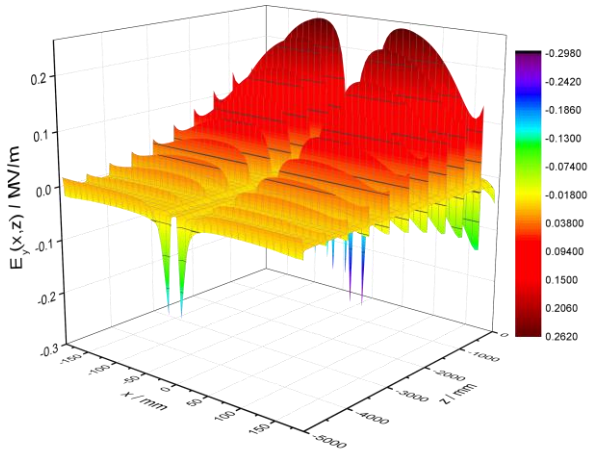

Fig. 16. $E_y(x, z)$ distribution in the series SCBM area.

In this section, 5 cases of series SCBM are tested, as shown in Table 2. There are 10 SCBMs connected for case I and case II, and the length of each SCBM is L_1=450 mm and the distance between two neighbouring SCBMs are all L_2=50 mm for case I, while L_1= 350 mm and L_2=150 mm for case II. The connected SCBMs number is 8 for case III and case IV, and L_1=475 mm and L_2 =150 mm for case III, while L_1=275 mm and L_2=250 mm for case IV. Additionally, the extreme condition case V, where L_2 =0 mm, is also included as for comparison.

To analyse series SCBM performance, we firstly monitored field distribution $E_h(x, z)$ in SCBM plane of case I, which is calculated by (5). In Fig. 14 is graphed $E_h(x, z)$ in the series SCBM area, where $x \in$ (-190 mm, 190 mm), $z \in$ (-5000 mm, 0 mm). And Fig.15 graphs $E_y(x, z)$ in the series SCBM area.

Firstly, it can be seen that the electric field in each SCBM is much lower than that in the space area between SCBMs, which means all the SCBMs play positive role

in flowing lightening current to the ground. Secondly, electric field E_h and E_y amplitude decreases from the lifting line side to the opposite side in the series SCBM length direction. Thirdly, electric field E_h increases from the central part of series SCBM to the outer sides in the width direction. Fourthly, from the comparison of Fig. 15 with Fig. 16, it can be seen that the electric field in Fig. 16 is much larger than that in Fig. 16, which means that horizontal direction is the main direction that lightning current flows. Thus, it is suggested to use cuboid SCBM horizontally buried to allow lightning current flow horizontally in mountain areas, where only a thin low resistivity soil is covered and high resistivity rocks buried below.

Table 3: Steady resistance of 5 Series SCBM

	Case I	**Case II**	**Case III**	**Case IV**	**Case V**
L (mm)	4500	3500	3800	2200	5000
Resistance	20.35 Ω	21.41 Ω	21.18 Ω	22.52 Ω	19.69 Ω

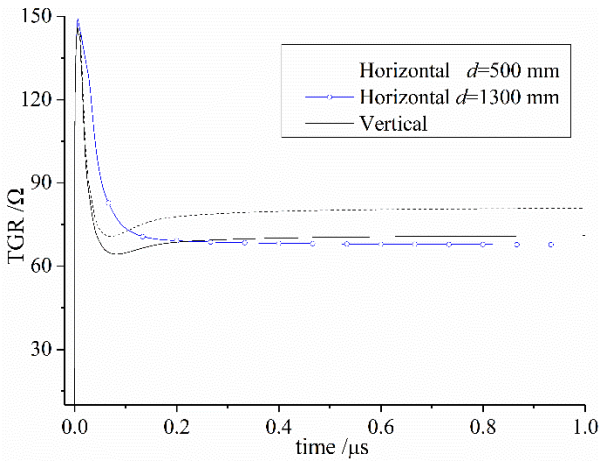

Fig. 17. TGR of 5 cases series SCBM.

From both Fig. 15 and Fig. 16, it can be seen that the electric field component in space areas between SCBMs is very high, which means closely buried two SCBMs will affect each other in flowing lightning current. Further, it can be concluded that the SCBMs have not performed sufficiently to flow lighting current to the ground when there was only 50 mm between the two neighbouring SCBMs.

Additionally, TGRs of the 5 cases series SCBM are also calculated and graphed in Fig. 17. In Table 3 is listed the steady resistance of the 5 cases, where the total SCBMs length given by $L=n\times L_1$ is also compared.

In Fig. 17, case V is used as a reference where the distance between neighbouring SCBMs L_2 is reduced to 0, which means one 5 m long SCBM is involved. From Fig. 17, it is clear that TGRs from 0 to 0.05 μs of the 5 cases are nearly the same, but transient resistance varies after 0.05 μs. The resistance of case I to case IV are both larger than that of case V after 0.05 μs, however the difference is not very significant. From Table 3, it can be seen that more SCBM usage would result in a lower steady resistance. Compared with a 5 m long SCBM used for case V, only 44% SCBM is used for case IV and there is only a 2.83 Ω more steady resistance gained. Thus, it can be concluded that it is not needed to connect the SCBMs one by one tightly in series SCBM, and some distances is allowed without dramatically increase the resistance but can dramatically reduce SCBM usage.

IV. CONCLUSIONS

In this paper, some improvements are proposed based on FDTD simulation for SCBM in grounding systems. Firstly, the SCBM can be made into several layers with conductivity decreasing gradually from inner layer to outer layer, and smooth conductivity reduction between neighbouring layers would lead to a better grounding performance. Secondly, SCBM shape has significant effect on its grounding resistance and cuboid shape is a more efficient shape for SCBM which can result in smaller grounding resistance at similar high conductivity material usage. Thirdly, holes effect on SCBM's performance is studied, and it is found both square and round holes can be made on the SCBM main body when producing the SCBM, which will affect the SCBM performance slightly. Fourthly, from comparison of SCBM buried position effect on TGR, it suggested to bury SCBM vertically when ground soil permits, otherwise bury SCBM horizontally and greater depth of the horizontal buried SCBM would result in smaller resistance. Lastly, series SCBM performance is analysed and results show it is not needed to connect the SCBMs one by one tightly in series SCBM, and some distance is allowed without dramatically increasing grounding resistance.

REFERENCES

[1] M. E. M. Rizk, M. Lehtonen, Y. Baba, S. Abulanwar, "Performance of large-scale grounding systems in thermal power plants against lightning strikes to nearby transmission towers," *IEEE Trans. on Elecgtromagn. Compt.*, vol. 61, no. 2, pp. 400-408, 2019.

[2] J. He, G. Yu, J. Yuan, R. Zeng, B. Zhang, J. Zou, and Z. Guan, "Decreasing grounding resistance of substation by deep-ground-well method," *IEEE Trans. on Power Del.*, vol. 20, no. 2, pp. 738-794, 2005.

[3] A. M. R. Martins, S. J. P. S. Mariano, M. R. A. Calado, and J. A. M. Felippe de Souza, "The sinusoidal ground electrode: Theory and case study results," *Applied Computational Electromagnetics*

Society Journal, vol. 31, no. 3, pp. 261-269, 2016.

[4] W. Zhou, G. Wu, X. Cao, and S. Li, "Research on effects between grounding module and grounding resistance," *Transmission and Distribution Conf. and Exposition*, T&D. *IEEE/PES*, pp. 1-4, 2008.

[5] Y.-Y. Chung, "Low-resistance carbon grounding module and method for manufacturing the same," *U.S. Patent, 20120293300 A1*, Nov. 2012.

[6] S. Visacro and G. Rosado, "Response of grounding electrodes to impulsive currents: An experimental evaluation," *IEEE Trans on Electromagn. Compat.*, vol. 51, no. 1, pp. 161-164, 2009.

[7] S. Sekioka, T. Sonoda, and A. Ametani, "Experimental study of current-dependent grounding resistance of rod electrode," *IEEE Trans. on Power Del.*, vol. 20, no. 2, pp. 1569-1576, 2005.

[8] H. Wan, X. Wang, Y. Chen, X. Pan, and X. Lu, "An extension of Cooray-Rubinstein formula on the calculation of horizontal electric field from inclined lightning channel," *Applied Computational Electromagnetics Society Journal*, vol. 33, no. 5, pp. 537-545, 2018.

[9] M. O. Goni, E. Kaneko and A. Ametani, "Simulation of lightning return stroke currents and its effect to nearby overhead conductor," *Applied Computational Electromagnetics Society Journal*, vol. 28, no. 1, pp. 469-477, 2009.

[10] M. Tsumura, Y. Baba, N. Nagaoka, and A. Ametani, "FDTD simulation of a horizontal grounding electrode and modeling of its equivalent circuit," *IEEE Trans Electromagn. Compat.*, vol. 48, no. 4, pp. 817-825, 2006.

[11] B. Li, Y. Du, and M. Chen, "An FDTD thin-wire model for lossy wire structures with noncircular cross section," *IEEE Trans. on Power Del.*, vol. 33, no. 6, pp. 3055-3064, 2018.

[12] A. Taflove and S. C. Hagness, *Computational Electrodynamics: The Finite-Difference Time-Domain Method*. Artech House, 3rd ed., 2005.

[13] X.-K. Wei, W. Shao, X. Ding, and B.-Z. Wang, "Efficient sub-gridded FDTD for three-dimensional time-reversed electromagnetic field shaping," *Applied Computational Electromagnetics Society Journal*, vol. 33, no. 8, pp. 828-836, 2018.

[14] Z. Sun, L. Shi, Y. Zhou, B. Yang, and W. Jiang, "FDTD evaluation of LEMP considering the lossy dispersive ground," *Applied Computational Electromagnetics Society Journal*, vol. 33, no. 1, pp. 7-14, 2018.

[15] R. Xiong, B. Chen, B.-H. Zhou, and C. Gao, "Optimized programs for shaped conductive backfill material of grounding systems based on the FDTD simulations," *IEEE Trans. on Power Del.*, vol. 29, no. 4, pp. 1744-1751, 2014.

[16] J. A. Roden and S. D. Gedney, "Convolution PML (CPML): An efficient FDTD implementation of the CFS-PML for arbitrary media," *Microw. Opt. Technol. Lett.*, vol. 27, no. 5, pp. 334-339, 2000.

[17] R. Xiong, B. Chen, C. Gao, Y. Yi, and W. Yang, "FDTD calculation model for the transient analyses of grounding systems," *IEEE Trans. on Electromagn. Compat.*, vol. 56, no. 5, pp. 1155-1162, 2014.